

A Synthetic DNA Walker for Molecular Transport

Jong-Shik Shin[†] and Niles A. Pierce^{*,†,‡}

Departments of Bioengineering and Applied & Computational Mathematics, California Institute of Technology, Pasadena, California 91125

Received April 27, 2004; E-mail: niles@caltech.edu

Biological systems have evolved motor proteins programmed to perform intracellular transport powered by ATP hydrolysis.^{1,2} Synthetic machines have accomplished mechanical switching between stable states in response to external stimuli,^{3–7} suggesting the promise of constructing a synthetic transport device that mimics the linear movement of motor proteins. Sherman and Seeman recently demonstrated a bipedal DNA walker that locomotes in an inchworm fashion, with one foot always trailing the other.⁸ Here, inspired by kinesin movement along a microtubule,^{9,10} we demonstrate a processive bipedal DNA nanomotor that moves by advancing the trailing foot to the lead at each step. Real-time monitoring of walker movement is achieved via multiplexed fluorescence quenching.

The system has four components (Table 1): a walker (W), a track (T), attachment fuel strands (A), and detachment fuel strands (D). The walker consists of two partially complementary oligonucleotides, with a 20-bp helix joining two single-stranded legs (each 23 bases). The track, constructed of six oligonucleotides, has four protruding single-stranded branches (each 20 bases) separated by 15-bp scaffold helices. Neighboring branches run in opposite directions, so spacing of 1.5 helical turns places all branches on the same side of the track approximately 5 nm apart (Figure 1).

As shown in Figure 1, the walker strides along the track under the external control of A and D strands. An A strand specifically anchors the walker to a branch by forming helices with the corresponding leg (18-bp) and branch (17-bp). Single-stranded hinges adjacent to either end of these helices (underlined in Table 1) provide flexibility for adopting different conformations depending on the fuel species that are present. When both legs are bound to the track, the trailing leg is released using a D strand that nucleates with the perfectly complementary A strand at a 10-base overhang and then undergoes a strand displacement reaction to produce duplex waste and free the walker leg for the next step.

Sequence selection for these system components represents a multi-objective optimization problem requiring the conditional stability of many different secondary structures, depending on the subsets of strand species that are considered. Primary sequence design was performed using automated sequence selection software¹¹ to minimize sequence symmetry¹² while maximizing the probability¹³ of adopting a compound secondary structure involving all the strands in the walker system. Subsequent secondary structure prediction¹⁴ for various pairs of strands revealed a small number of undesirable interactions, which were eliminated by slight sequence modifications.

To detect walker locomotion, all four branches are end-labeled with different dyes and the two walker legs are end-labeled with quenchers (Table 1) to allow monitoring of fluorescence changes associated with each dye. Proper monomeric association between the walker and track is demonstrated by examining intermediates

Table 1. DNA Sequences for the Walker System^{a,b}

Walker strands (W)	
W1	5'-GGCTGGTTTCTGCTCTCTAGTTCGCGAGGTGCAATCTCCTATC-3'-BHQ1
W2	IBRQ-5'-GTCTGGGATGCTGGATACTGAACCTAGAGAGCAGAAACCAGCC-3'
Track strands (T)	
T1	HEX ^c -5'-GCTGTACTTTGGTTACTGAAAGGGAGTGGCTCGGA-3'
T2	5'-TCCGAGCCACTCCCTGGACACCATCTACAAACTTGTATGGGACGTAGCGT-3'-Cy5
T3	FAM ^d -5'-TCCACATCGGACTGTGAATGCAAGACACGTTACTTGTAGATGGTGTCC-3'
T4	5'-GTAACGTGCTTTGCTCTCAAACATACGCTCTTCATGGCATTTCGTACCA-3'-Texas Red
T5	5'-AACTCTTAGCCAAAGATCGTAAGCGTATGTTTGA-3'
T6	5'-TACGATCTTGGCTAAGAGTT-3'
Attachment strands (A)	
A1	5'-AGTAACCAAGTACAGCACTGCGATAGGAGATTGCACCTCCAATTTACCC-3'
A2	5'-GACTGTTACGGTATCCAGCATCCGACGCTCAACGCTACGTCACATACA-3'
A3 ^e	5'-ACAGAGTCCGATGTGGAAGTCAGATAGGAGATTGCACCTCATCATTGTCG-3'
A4 ^e	5'-GGATCAGTTAGTATCCAGCATCCAGACCTAAGTGGTGACGAATGCCATG-3'

^a Color use is consistent in all graphics. ^b Sequences synthesized, labeled, and purified by Integrated DNA Technologies, Inc. ^c Hexachlorofluorescein. ^d 6-Carboxyfluorescein. ^e Strands not depicted in Figure 1.

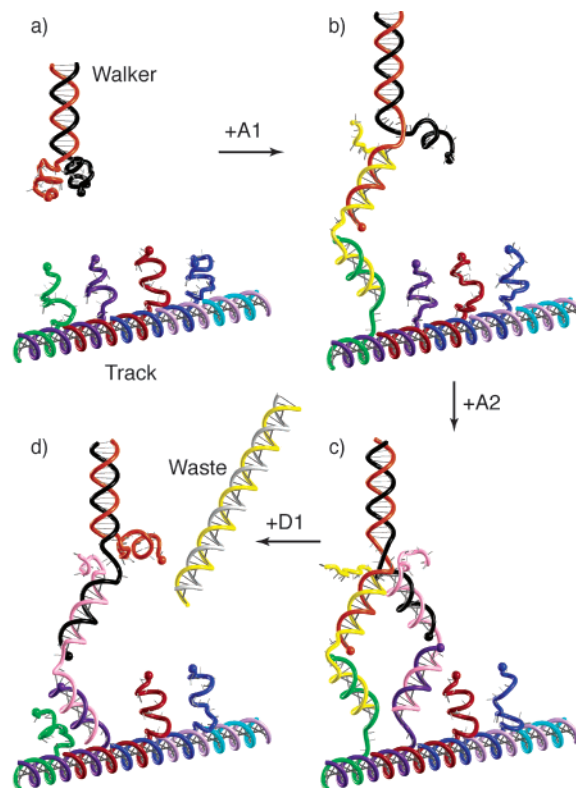


Figure 1. Schematic of walker locomotion. Colored spheres represent dyes (HEX, green; Cy5, purple; FAM, red; Texas Red, blue) and quenchers (BHQ1, orange; IBRQ, black) for detecting walker movement. The diagrams depict (a) unbound walker, (b) walker attached to branch 1, (c) walker attached to branches 1 and 2, and (d) walker released from branch 1 to yield duplex waste.

during two forward steps using non-denaturing gel electrophoresis visualized with two different fluorescent scans (Figure 2). The major band, corresponding to fully assembled track (lane 1),

[†] Department of Bioengineering.

[‡] Department of Applied & Computational Mathematics.

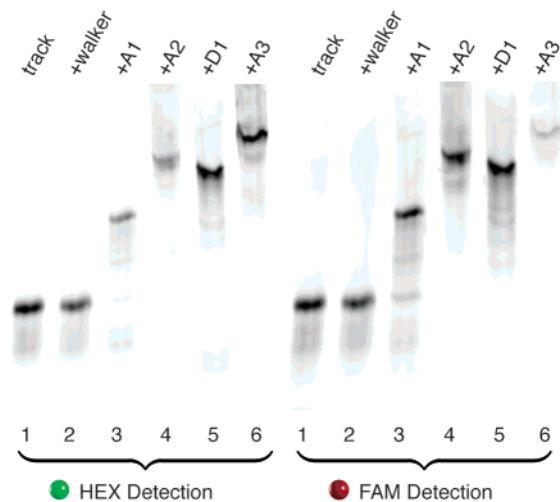


Figure 2. Non-denaturing polyacrylamide gel analysis. This figure is a composite of two images obtained by different fluorescent scans of the same gel (532 nm excitation and a 555 nm cutoff filter to detect HEX, and 488 nm excitation and a 30 nm band-pass filter centered at 530 nm to detect FAM). Equimolar amounts of walker and fuel (1 μ M) were successively added to the track in TSE buffer (10 mM Tris, 150 mM NaCl, 1 mM EDTA, pH 7.5) followed by 1 h incubation at 37 $^{\circ}$ C. Gel electrophoresis was performed in 1 \times TBE buffer at 50 V and 4 $^{\circ}$ C with 6.7% acrylamide.

is accompanied by minor bands representing partially formed tracks. These partial tracks result from slight discrepancies in stoichiometry between the six track species and lead to the observation of minor bands during subsequent stages of the experiment. The track does not exhibit nonspecific interactions with the walker (lane 2). Anchoring of the walker and subsequent translation results in less mobile intermediates (lanes 3–6). The band intensities of these intermediates are consistent with the expected position of the walker for both wavelength scans. For HEX detection, there is a reduction in band intensity for lanes 3 and 4 relative to lanes 1, 2, 5, and 6. For FAM detection, there is a reduction in band intensity for lane 6 relative to lanes 1–5. The absence of empty track during the operation demonstrates the processivity of walker movement (i.e., at least one leg stays bound to the track).

Real-time monitoring of walker movement was carried out by multiplexed fluorescence quenching measurements (Figure 3). Traversing the track from one end to the other and back, the fluorescent signal from each branch responds specifically to the addition of cognate fuel strands, illustrating high fidelity in controlling walker movement with nanoscale precision.

We have demonstrated a synthetic molecular walker that mimics the bipedal gait of kinesin. The present 5 nm step size is smaller than the 8 nm stride of kinesin on a microtubule,^{9,10} and is tunable by adjusting the design of the track scaffold. The walker system comprises 16 strand species containing 726 nucleotides, which encode conditional affinity and specificity for different walker conformations, depending on the external stimulus. Generalization to much longer tracks should be possible by attaching branches to more rigid substrates such as planar¹⁵ or tubular¹⁶ DNA crystals. In this setting, specific directional control should be achievable without increasing the number of attachment and detachment fuel species by arranging branch species with a periodicity of four. While the present walker transports two quenchers covalently linked to the feet, transport of non-covalently bonded molecular cargo should also be realizable by generalizing the walker structure to incorporate an aptamer that binds the cargo ligand with high affinity and specificity.¹⁷ Ultimately, the development of an efficient catalytic DNA fuel delivery mechanism¹⁸ should enable the rational design

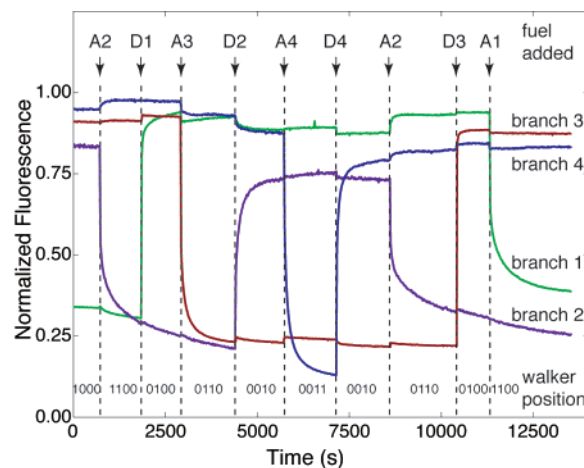


Figure 3. Multiplexed real-time fluorescence monitoring. Track (0.5 μ M) was preincubated in TSE buffer with equimolar walker and A1 for 4 h at room temperature (100 μ L working volume). Equimolar amounts of A and D fuel strands were successively added from 100 \times stocks and mixed by rapid pipetting. Excitation and emission wavelengths were 495/520 nm for FAM, 538/555 nm for HEX, 598/617 nm for Texas Red, and 648/668 nm for Cy5 with 4 nm bandwidths. Fluorescence intensities are normalized by the initial track values. The binary digits at the bottom represent the location of the walker on branches 1–4 (0 for unbound state, 1 for bound state).

of a completely artificial DNA walker that locomotes autonomously, allowing detailed programming of a motor protein mimic.

Acknowledgment. We thank the Winfree laboratory at Caltech for the use of their fluorescent gel scanner. The following research support is gratefully acknowledged: DARPA and the Air Force Research Laboratory under agreement F30602-01-2-0561, the Ralph M. Parsons Foundation, and the Charles Lee Powell Foundation.

Supporting Information Available: Materials and methods; independence of fluorescence signals. This information is available free of charge via the Internet at <http://pubs.acs.org>.

References

- (1) Vale, R. *Cell* **2003**, *112*, 467–480.
- (2) Schliwa, M.; Woehlke, G. *Nature* **2003**, *422*, 759–765.
- (3) Mao, C.; Sun, W.; Shen, Z.; Seeman, N. C. *Nature* **1999**, *397*, 144–146.
- (4) Yurke, B.; Turberfield, A.; Mills, A. P., Jr.; Simmel, F.; Neumann, J. *Nature* **2000**, *406*, 605–608.
- (5) Yan, H.; Zhang, X.; Shen, Z.; Seeman, N. C. *Nature* **2002**, *415*, 62–65.
- (6) Leigh, D.; Wong, J.; Dehez, F.; Zerbetto, F. *Nature* **2003**, *424*, 174–179.
- (7) Badjic, J.; Balzani, V.; Credi, A.; Silvi, S.; Stoddart, J. *Science* **2004**, *303*, 1845–1849.
- (8) Sherman, W.; Seeman, N. C. *Nano Lett* **2004**, *4*, 1203–1207.
- (9) Block, S. *Cell* **1998**, *93*, 5–8.
- (10) Vale, R.; Milligan, R. *Science* **2000**, *288*, 88–95.
- (11) Dirks, R.; Pierce, N. A. *J. Comput. Chem.* **2003**, *24*, 1664–1677.
- (12) Seeman, N. C. *J. Theor. Biol.* **1982**, *99*, 237–247.
- (13) Hofacker, I.; Fontana, W.; Stadler, P.; Bonhoeffer, L.; Tacker, M.; Schuster, P. *Chem. Monthly* **1994**, *125*, 167–188.
- (14) Zuker, M. *Nucleic Acids Res.* **2003**, *31*, 3406–3415.
- (15) Winfree, E.; Liu, F.; Wenzler, L.; Seeman, N. C. *Nature* **1998**, *394*, 539–544.
- (16) Liu, D.; Park, S.; Reif, J.; LaBean, T. *Proc. Natl. Acad. Sci. U.S.A.* **2004**, *101*, 717–722.
- (17) Hermann, T.; Patel, D. *Science* **2000**, *287*, 820–825.
- (18) Turberfield, A. J.; Mitchell, J.; Yurke, B.; Mills, A. P., Jr.; Blakey, M.; Simmel, F. *Phys. Rev. Lett.* **2003**, *90*, 118102.

JA047543J